

# A lattice refinement scheme for finding periodic orbits

B.I. Henry\*

S.D. Watt\*

S.L. Wearne\*

(Received 7 August 2000)

## Abstract

A lattice refinement scheme based on the principle of linearized stability is introduced to locate periodic orbits in a two-dimensional map. The method locates all periodic orbits of a specified order within a given starting window and it can be equally well applied when the map is only known implicitly, e.g., as a two-dimensional surface of section arising from a three-dimensional flow. Periodic orbits in the

---

\*Department of Applied Mathematics, School of Mathematics, University of New South Wales, Sydney NSW 2052, AUSTRALIA. <mailto:bihenry@maths.unsw.edu.au>

<sup>0</sup>See <http://anziamj.austms.org.au/V42/CTAC99/Henr> for this article and ancillary services, © Austral. Mathematical Soc. 2000. Published 27 Nov 2000.

Hénon Map, the Predator-Prey Map, the Rössler Flow, and the Lorenz Flow are constructed as illustrations of the method.

## Contents

<b>1 Introduction</b>	<b>C736</b>
<b>2 Lattice Refinement Scheme</b>	<b>C738</b>
<b>3 Numerical Examples</b>	<b>C743</b>
<b>References</b>	<b>C750</b>

## 1 Introduction

In recent years there has been much interest in accurately computing unstable periodic orbits of chaotic dynamical systems. For example in Quantum Mechanics a weighted sum over periodic orbits yields quantum mechanical energy level spacings [1] and in Statistical Mechanics a different sum over unstable periodic orbits, weighted according to the values of their Liapunov exponents, can be used to calculate thermodynamic averages [2].

A popular brute force method for finding  $p$ -periodic orbits of chaotic

dynamical systems is to search a long chaotic trajectory for near recurrences between phase space points after  $p$  crossings on a surface of section and then to average over the near recurrences. The method introduced in this paper, while motivated by the problem of finding periodic orbits in three-dimensional flows, provides a systematic method for finding periodic orbits in general two-dimensional maps.

The method utilizes the principle of linearized stability to search an initial trial lattice for a lattice cell containing a near recurrence. It then uses a succession of lattice refinements based on the principle of linearized stability to converge towards exact recurrence points. We have restricted our attention to finding  $p$ -periodic orbits of two-dimensional maps (and three dimensional flows) however the method could be readily extended to finding periodic orbits in higher dimensional systems.

Our scheme is similar to other variants of Newton's method (see for example, [6, Appendix E] and [7, Chapter 10]) in that it utilizes information about the local dynamics of the map to make further refinements. An alternative method, the "topological degree" method [3, 4, 5], makes refinements using a generalized bisection method based on function evaluations at the vertices of polyhedra. Key advantages of the lattice refinement scheme are: (i) it systematically searches for all periodic orbits in a given starting window; and (ii) it does not need good starting approximations to locate the periodic orbits. In general, other schemes require 'good' initial guesses to find a single periodic orbit. In the variants of Newton's method a good initial guess is one in which the local dynamics in the vicinity of the guess are similar to

the local dynamics in the vicinity of the single periodic orbit of interest. In the case of the topological degree method a good initial guess is a polyhedra that contains only the one periodic orbit in its interior. These methods may be preferred when sufficiently good guesses are available.

## 2 Lattice Refinement Scheme

The first step in the lattice refinement procedure is to identify a starting window  $\{(x, y) \mid x_{\min} \leq x \leq x_{\max}; y_{\min} \leq y \leq y_{\max}\}$ . Some knowledge of the dynamical system would assist in this choice however the speed of the algorithm makes it feasible to investigate large initial windows without *a priori* knowledge. In the case of a three-dimensional flow this starting window would be a region on a two-dimensional Poincaré surface of section that is transverse to the flow. The search for periodic orbits is confined to the starting window.

The next step is to cover the window with a uniform rectangular lattice of  $n \times m$  cells by defining lattice vertices  $(x_{j,k}, y_{j,k})$ :

$$\begin{aligned}x_{j,k} &= x_{\min} + (j - 1)dx, & j &= 1, \dots, n + 1 \\y_{j,k} &= y_{\min} + (k - 1)dy, & k &= 1, \dots, m + 1\end{aligned}$$

where  $dx = (x_{\max} - x_{\min})/n$  and  $dy = (y_{\max} - y_{\min})/m$ . Now integrate the equations of motion using each of the lattice vertices as initial conditions and

record the evolved co-ordinates of the lattice vertices  $(x'_{j,k}, y'_{j,k})$  at the next intersection with the surface of section. The evolved lattice vertices (which can be located accurately using Hénon's method [8] if the map is only defined implicitly as a Poincaré map) are related to the original lattice vertices by

$$(x'_{j,k}, y'_{j,k}) = M(x_{j,k}, y_{j,k}).$$

Our aim is to find the fixed point  $(\bar{x}, \bar{y})$  of the map  $M$ . If  $M$  is a Poincaré map then this fixed point might correspond to a fixed point of the flow or a point on a period-one orbit.

For each lattice cell, the initial lattice vertices and the evolved vertices can be used to determine four affine transformations  $T$  which approximate the map  $M$ . In general  $T$  is defined by

$$\begin{pmatrix} x' \\ y' \end{pmatrix} = \underline{\underline{A}} \begin{pmatrix} x \\ y \end{pmatrix} + \underline{b} = \begin{pmatrix} a & b \\ c & d \end{pmatrix} \begin{pmatrix} x \\ y \end{pmatrix} + \begin{pmatrix} e \\ f \end{pmatrix}. \quad (1)$$

A particular affine transformation for a given cell is uniquely specified by the transformation of three of the vertices. As an example, for the lattice cell with vertices

$$[(x_{j,k}, y_{j,k}), (x_{j+1,k}, y_{j+1,k}), (x_{j,k+1}, y_{j,k+1}), (x_{j+1,k+1}, y_{j+1,k+1})],$$

the affine transformation that takes

$$[(x_{j,k}, y_{j,k}), (x_{j+1,k}, y_{j+1,k}), (x_{j,k+1}, y_{j,k+1})]$$

to

$$[(x'_{j,k}, y'_{j,k}), (x'_{j+1,k}, y'_{j+1,k}), (x'_{j,k+1}, y'_{j,k+1})]$$

has

$$\begin{aligned} a &= (x'_{j+1,k} - x'_{j,k})/\alpha \\ b &= (x'_{j,k+1} - x'_{j,k})/\beta \\ c &= (y'_{j+1,k} - y'_{j,k})/\alpha \\ d &= (y'_{j,k+1} - y'_{j,k})/\beta \\ e &= x'_{j,k} + x_{j,k}(x'_{j,k} - x'_{j+1,k})/\alpha + y_{j,k}(x'_{j,k} - x'_{j,k+1})/\beta \\ f &= y'_{j,k} + x_{j,k}(y'_{j,k} - y'_{j+1,k})/\alpha + y_{j,k}(y'_{j,k} - y'_{j,k+1})/\beta. \end{aligned}$$

The constants  $\alpha$  and  $\beta$  denote the lattice spacing in the  $x$  and  $y$  directions respectively. Each of the affine transformations for a given cell has a fixed point  $(x^*, y^*)$  given by

$$\begin{pmatrix} x^* \\ y^* \end{pmatrix} = (\underline{I} - \underline{A})^{-1} \underline{b} = \begin{pmatrix} \frac{e-ed+bf}{1-d-a+ad-bc} \\ \frac{f-fa+ce}{1-d-a+ad-bc} \end{pmatrix}. \quad (2)$$

The four affine transformations yield different fixed points in general. However if  $M$  is of the form

$$\begin{aligned} x' &= f_1(x) + g_1(y) \\ y' &= f_2(x) + g_2(y) \end{aligned} \quad (3)$$

where  $f_{1,2}(x)$  and  $g_{1,2}(y)$  are arbitrary functions then each of the four affine maps  $T$  for a given cell is identical. A linear map is a special case of Equation (3) where  $f_{1,2}(x)$  and  $g_{1,2}(y)$  are linear functions.

In general fixed points of the affine maps may or may not approximate fixed points  $(\bar{x}, \bar{y})$  of the map  $M$ . Suppose however that fixed points of  $M$  are located inside the initial window. From the principle of linearized stability (see for example, [9, Chapters 4,5]) it follows that  $M$  can be approximated by its linearization in the vicinity of fixed points. Hence the fixed points identified by the affine transformations of lattice cells provide crude approximations to the fixed points of  $M$ . Improved approximations are then possible by calculating fixed points of affine transformations of smaller cells in the neighbourhood of the crude approximations. Fixed points of linearizations with increasingly smaller cells in the neighbourhood of these revised fixed point approximations provide increasingly better approximations. Eventually the process identifies a cell containing the fixed points of all four affine transformations. This suggests that the identified cell contains the fixed point of the map.

We use the above observations as the basis for an algorithm to determine a cell which contains a fixed point of  $M$ . From the original lattice coordinates and the evolved lattice co-ordinates we identify those cells which contain fixed points of the linearizations - considering all four affine transformations for all cells. Possible candidate fixed points of  $M$  are now specified to within the size of these selected cells. An improved estimate for the putative fixed point  $(\bar{x}, \bar{y})$  in a cell  $\gamma$  can be obtained by repeating the procedure, but this time using the vertices of the cell  $\gamma$  to replace the previous values of  $(x_{\min}, y_{\min})$  and  $(x_{\max}, y_{\max})$ . Proceeding in this iterative fashion refined estimates of the putative fixed points of  $M$  and thus the period-one orbit can be obtained. This process can be continued until the lattice cell size is

smaller than a specified tolerance  $\epsilon$ . At each stage of the process the original grid points and the putative fixed points are all evolved to determine if they are true fixed points to within the specified tolerance  $\epsilon$ . The numerical estimates of the fixed points are obtained as an average of the putative fixed points  $(x^*, y^*)$  and the evolved putative fixed points  $(x'^*, y'^*)$  that satisfy the condition  $d(x^*, y^*) \leq \epsilon$  where the orbital closure error,  $d(x^*, y^*)$ , is defined by

$$d(x^*, y^*) = \sqrt{(x'^* - x^*)^2 + (y'^* - y^*)^2}.$$

The linear test may fail to yield a putative fixed point for a given cell which does contain a fixed point of the map  $M$  if the lattice size is too large to approximate  $M$  by affine maps. To address this possibility the procedure could be repeated using larger values for  $n$  and  $m$  or a smaller starting window. Our experience suggests that a reduction in window size is to be preferred over increases in  $n$  and  $m$  since such increases significantly reduce the speed of the algorithm. Furthermore the limiting values  $n = (x_{\max} - x_{\min})/\epsilon$  and  $m = (y_{\max} - y_{\min})/\epsilon$  are equivalent to a brute force search. In all of the examples below our choice  $n = m = 3$  reveals all possible fixed points within the starting windows.

Another possible problem may arise if one of the lattice vertices is an exact fixed point. It is a simple matter to identify such possibilities in any given lattice and then to remove the problem, for example by reselecting  $n$  and  $m$  to provide a new incommensurate lattice.

Higher order periodic orbits can be found in an analogous fashion. First

iterate the map  $p$  times using each of the lattice points  $(x_{j,k}, y_{j,k})$  as initial conditions and record the evolved co-ordinates of the lattice points  $(x'_{j,k}, y'_{j,k})$  after the  $p$ th iteration. In a flow the implicit map is iterated  $p$  times by numerically integrating the equations of motion and finding the  $p$ th intersection with the surface of section. In either case the evolved lattice points are related to the original lattice points by

$$(x'_{j,k}, y'_{j,k}) = M^p(x_{j,k}, y_{j,k})$$

The procedure described above for finding the fixed points of  $M$  can be used to find the fixed points of  $M^p$ . The fixed points of  $M^p$  that are not also fixed points of  $M^q$  where  $q < p$  are points on a  $p$ -periodic orbit.

## 3 Numerical Examples

The lattice refinement scheme for finding periodic orbits can be implemented very efficiently using recursive programming. In the numerical results reported below we implemented the method using recursive subroutine calls in FORTRAN 90.

To illustrate the lattice refinement scheme we have calculated periodic orbits in:

1. the Hénon Map [10], a special case of Equation (3),

$$\begin{aligned}x' &= y + 1 - ax^2 \\y' &= bx\end{aligned}$$

with  $a = 1.4$  and  $b = 0.3$ ;

2. the Predator-Prey Map [11]

$$\begin{aligned}x' &= ax(1 - x) - xy \\y' &= bxy\end{aligned}$$

with  $a = 3.6545$ ,  $b = 3.226$ ;

3. the Rössler Flow [12] (the  $y$  and  $z$  variables have been interchanged in our representation of the Rössler flow for ease of presentation)

$$\begin{aligned}\dot{x} &= -y - z \\ \dot{y} &= b + y(x - c) \\ \dot{z} &= x + az\end{aligned}$$

with  $a = 0.2$ ,  $b = 0.2$ ,  $c = 5.7$  and surface of section  $z = 0$ ; and

4. the Lorenz Flow [13]

$$\begin{aligned}\dot{x} &= \sigma(y - x) \\ \dot{y} &= rx - y - xz \\ \dot{z} &= xy - bz\end{aligned}$$

with  $\sigma = 10$ ,  $r = 28$ ,  $b = 8/3$  and surface of section  $z = 27$ .

Figure 1 shows cells that were explored under subsequent lattice refinements in the search for the period one orbit in each of the above systems using a tolerance of 0.001, an initial window  $x \in [-9, 9]$  and  $y \in [-9, 9]$  and a  $3 \times 3$  lattice.

The lattice refinement scheme was extremely efficient in the case of the Hénon Map where only one cell containing a spurious fixed point was examined.

The best numerical estimates of the fixed points (determined by the smallest orbital closure error  $d(x^*, y^*)$ ) are listed in Table 1. We have calculated the eigenvalues for each of the four affine transformations for each of the cells containing the period-one orbits. The average of the maximum eigenvalue from the four transformations and the average of the minimum eigenvalue from the four transformations are listed under the heading  $\langle \lambda^* \rangle$  in Table 1. The Liapunov exponents  $\Lambda$  can be readily found from  $\Lambda = \log(|\langle \lambda^* \rangle|)$ . In cases where exact results for the fixed points and eigenvalues can be calculated these exact results are also listed.

The numerical fixed points for the Rössler Flow are points on a period-one orbit. The complete periodic orbit is shown superimposed on the Rössler strange attractor in Figure 2(a). The numerical fixed points for the Lorenz Flow are actual fixed points of the flow rather than points on a period-one orbit. Indeed there is no period-one orbit of the Lorenz Flow that is transverse to the  $z = 27$  surface of section. The lowest order orbit is period-two in the sense that it pierces the surface of section twice before closure.

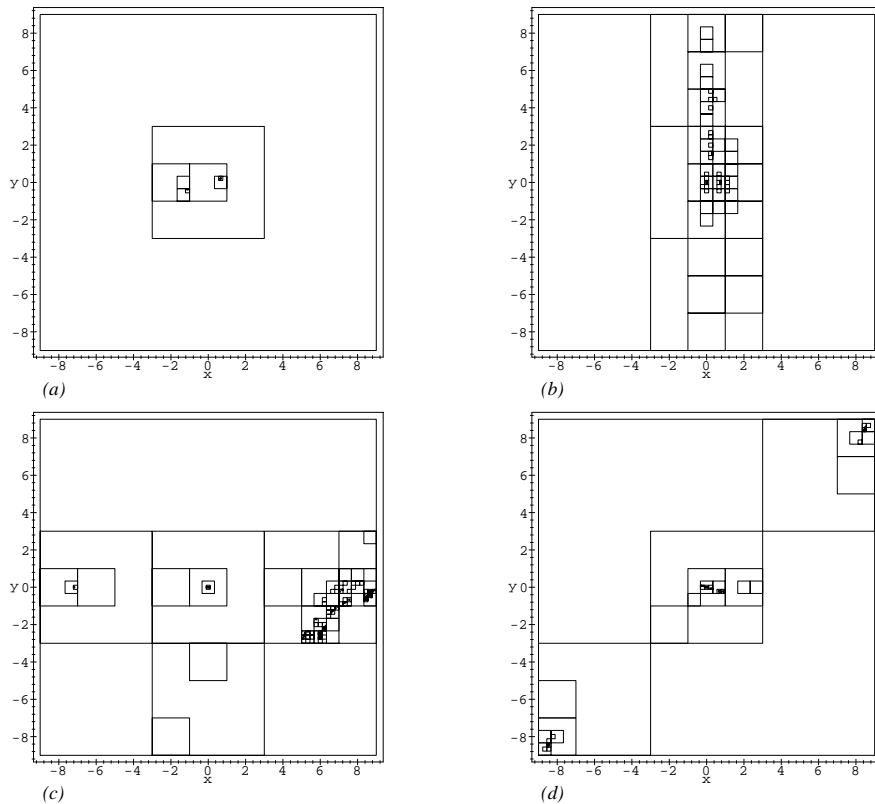


FIGURE 1: Cells that were explored using the lattice refinement scheme with a  $3 \times 3$  lattice for (a) the Hénon Map, (b) the Predator map, (c) the Rössler Flow (on  $z = 0$ ), and (d) the Lorenz Flow (on  $z = 27$ ).

TABLE 1: Numerical values  $Z^*$  and exact values ( $\bar{Z}$ ) of fixed points  $x, y$  and eigenvalues  $\lambda$ .

	$x^*$ ( $\bar{x}$ )	$y^*$ ( $\bar{y}$ )	$\langle \lambda^* \rangle$ ( $\bar{\lambda}$ )
Hénon Map	0.63135471 (0.63135447)	0.18940604 (0.18940634)	0.1560, -1.9228 (0.1559, -1.9237)
	-1.1313534 (-1.1313544)	-0.33940619 (-0.33940634)	3.2569, -0.09210 (3.2598, -0.09209)
Predator Map	0.72636465 (0.72636475)	$3.9 \times 10^{-6}$ (0.0)	2.3453, -1.6593 (2.343, -1.6545)
	0.3099849 (0.3099814)	1.521652 (1.521672)	$0.43304 \pm 1.0960I$ ( $0.43358 \pm 1.0958I$ )
	$4.3 \times 10^{-6}$ (0.0)	$-3.0 \times 10^{-6}$ (0.0)	$3.65449, 2.2 \times 10^{-12}$ (3.65450, 0.0)
Rössler Flow on $z = 0$	-7.211118	0.0155446	$7.3 \times 10^{-11}$ , -2.4027
Lorenz Flow on $z = 27$	-8.485281346 (-8.485281375)	-8.485281333 (-8.485281375)	
	8.485281356 (8.485281375)	8.485281352 (8.485281375)	

TABLE 2: Numerical values  $Z^*$  and exact values ( $\bar{Z}$ ) of period-two points  $x_1, x_2; y_1, y_2$  and eigenvalues  $\lambda$ .

	$x_1^*, x_2^*$ ( $\bar{x}_1, \bar{x}_2$ )	$y_1^*, y_2^*$ ( $\bar{y}_1, \bar{y}_2$ )	$\langle \lambda^* \rangle$ ( $\bar{\lambda}$ )
Hénon Map	-0.47579, 0.97579 (-0.47580, 0.97580)	0.292739, -0.14274033 (0.292740, -0.14274001)	-3.020, -0.02979 (-3.010, -0.02989)
Predator Map	0.3980158, 0.875625 (0.3980181, 0.875617)	$8.7 \times 10^{-6}$ , $-1.0 \times 10^{-5}$ (0.0, 0.0)	-2.0497, 3.6243 (-2.0463, 3.6269)
Rössler Flow on $z = 0$	-4.656809, -8.194643	0.019401, 0.014439	$2.8 \times 10^{-11}$ , -3.5113
Lorenz Flow on $z = 27$	+2.147367, -2.147367	-2.078048, +2.078048	1.3575, 0.0

We have also implemented the lattice refinement scheme to search for higher order periods. The results for period-two orbits are summarized in Table 2. Exact values for the Hénon Map and the Predator Map are listed for comparison.

The period-two orbits for the Rössler Flow and the Lorenz Flow are shown superimposed on the Rössler attractor and the Lorenz attractor in Figures 2(b) and 2(c) respectively. Figure 2(d) shows a period-five orbit for the Lorenz Flow identified using the lattice refinement scheme.

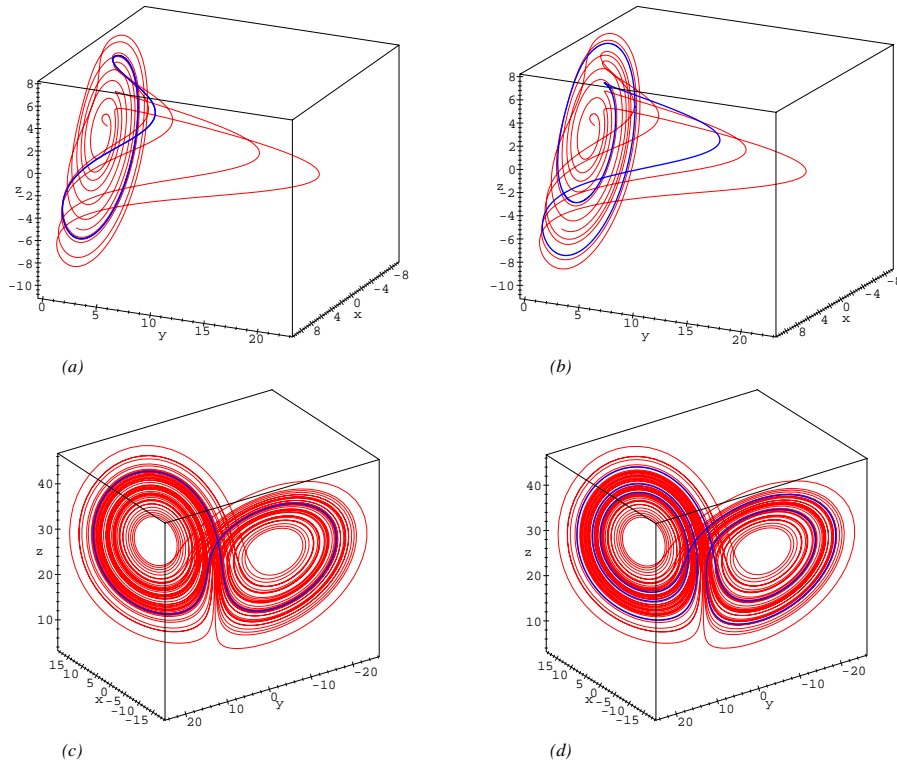


FIGURE 2: Periodic orbits in: (a), (b) the Rössler Flow on  $z = 0$ ; and (c), (d) the Lorenz Flow on  $z = 27$ . Initial conditions are (a)  $x = -7.211118$ ,  $y = 0.015544$ ; (b)  $x = -4.656809$ ,  $y = 0.019401$ ; (c)  $x = 2.147367$ ,  $y = -2.078048$ ; (d)  $x = 4.250440$ ,  $y = 1.008479$ . The blue lines show periodic orbits and the red lines show the strange attractor.

## References

- [1] M.C. Gutzwiller. *Chaos in Classical and Quantum Mechanics*. Springer-Verlag, New York, 1990.
- [2] G.P. Morriss and L. Rondoni. Chaos and its impact on the foundations of statistical mechanics. *Aust. J. Phys.*, 49:51–77, 1996.
- [3] M.N. Vrahatis and T.C. Bountis. An efficient method for computing periodic orbits in conservative dynamical systems. In J. Seimensis, editor, *Hamiltonian Mechanics*, pages 261–274. Plenum Press, New York, 1994.
- [4] M.N. Vrahatis. An efficient method for computing periodic orbits of nonlinear mappings. *J. Comput. Phys.*, 119:105–119, 1995.
- [5] L. Drossos, O. Ragos, M.N. Vrahatis, and T. Bountis. Method for computing long periodic orbits of dynamical systems. *Phys. Rev. E.*, 53:1206–1211, 1996.
- [6] C. Sparrow. *The Lorenz Equations: Bifurcations, Chaos and Strange Attractors*. Springer-Verlag, New York, 1982.
- [7] H.E. Nusse and J.A. Yorke. *Dynamics: Numerical Explorations*. Springer-Verlag, New York, 1994.
- [8] M. Hénon. On the numerical computation of Poincaré maps. *Physica*, 5D:412–414, 1982.

- [9] R. Grimshaw. *Nonlinear Ordinary Differential Equations*. CRC Press, Boca Raton, 1993.
- [10] M. Hénon. A two-dimensional mapping with a strange attractor. *Comm. Math. Phys.*, 50:69–77, 1976.
- [11] J. Maynard Smith. *Mathematical Ideas in Biology*. Cambridge University Press, London, 1968.
- [12] O.E. Rössler. An equation for continuous chaos. *Phys. Lett. A.*, 57:397–398, 1976.
- [13] E.N. Lorenz. Deterministic nonperiodic flow. *J. Atmos. Sci.*, 20:130–141, 1963.

C736 C736 C737 C737 C737 C737 C737 C739 C741 C744 C744 C744  
C744